Investigation and Optimization of Ti-6Al-4V Titanium Alloy in the Fine Grinding Process Using Cold Air Gun Coolant System

Chih-Chung Chou, Nun-Ming Liu, Ko-Ta Chiang*, Hsiao-Cheng Chang

Abstract

In this paper, a series of the surface machining experimentation using the cold air gun coolant system in the fine grinding process of Ti-6Al-4V titanium alloy was investigated for observing the machinability evaluation such as the quality of the ground surface, dimensions and shape precision. Meantime, the mathematical model was presented to model and analyze the machining parameters of the fine grinding process for the influences of the quality of the ground surface. A cold air gun coolant system was used in the experiments and produced a jet of compressed cold air in the air-cooling process during the metal grinding cutting process. Titanium alloys have found very wide application areas of aerospace, such as 3C industry, aviation industry, automotive, electric industry, medicine and dentistry due to their excellent corrosion resistance, lightweight, high fatigue strength, low thermal expansion, non-magnetismn, non-toxicity and mechanical properties. In this paper, the mathematical model was presented to model the machinability evaluation through the response surface methodology (RSM). The quadratic model of response surface methodology (RSM) associated with the sequential approximation optimization (SAO) method would be used to explain the relation of the finishing grinding process parameters and machining characteristic, and to find optimum values of machining parameters for the face cutting process of Titanium alloys.

Keywords: Cold air gun, Fine grinding process, Titanium alloy, Optimization

Chih-Chung Chou, Department of Mechanical Engineering, Hsiuping University of Science and Technology, Lecturer
Nun-Ming Liu, Department of Mechanical Engineering, Hsiuping University of Science and Technology, Assistant Professor
Ko-Ta Chiang, Department of Mechanical Engineering, Hsiuping University of Science and Technology, Professor. Corresponding author: kota@hust.edu.tw
Hsiao-Cheng Chang, Department of Mechanical Engineering, Hsiuping University of Science and Technology, Graduate student
Received 21 June 2016; accepted 23 August 2016

使用空氣槍冷卻系統於 Ti-6Al-4V 鈦合金的研磨精加工性能之分析與最佳化

周志忠、劉南明、江可達*、張孝崢

摘要

本研究中，進行一系列使用空氣槍冷卻系統於研磨精加工製程於鈦合金的表面加工實驗，藉此觀察其加工特性，如加工表面品質與尺寸、形狀精度等。同時進而建立數學模組用來建模與分析其研磨精加工製程的參數對其各項加工特性之影響，藉此觀察加工表面品質。同時進而建立數學模組用來與分析其研磨精製程的參數對加工表面品質之影響。一組冷空氣槍冷卻系統被在實驗過程中使用，用來產生壓縮冷空氣的氣流，在金屬研磨切削過程中作為空氣冷卻過程。由於鈦合金之材料特性其質輕、耐腐蝕、耐高溫、疲勞強度大、熱膨脹係數小、非磁性、非毒性等及其優異的機械性質，被廣泛運用於 3C 產業、航太工業、化學工業、電力設備、生醫工程、汽車工業等。使用反應曲面法的二階數學模組以及結合連續近似最佳法，獲得其二階數學模組用來解釋其使用空氣槍冷卻於研磨精加工製程加工參數與加工品質特性之相互影響關係，同時在品質特性中找出鈦合金的表面加工過程之最佳化加工參數的設定。

關鍵詞：建模、粉末混合放電加工、加工性能、反應曲面法

周志忠：修平科技大學機械工程系，講師
劉南明：修平科技大學機械工程系，助理教授
江可達：修平科技大學機械工程系，教授 *通訊作者：kota@hust.edu.tw
張孝崢：修平科技大學機械工程系，研究生
投稿日期：105 年 6 月 21 日　接受刊登日期：105 年 8 月 23 日

1. Introduction

Fine grinding processes are becoming the standard selection of manufacturing process, especially in the rapidly growing areas of automotive and aerospace industrial products. Grinding is an abrasive manufacturing process where material removals take place by randomly and stochastically distributed grains of grinding wheels [1]. Material removal rates resulting in a proportional increase in productivity have achieved machining requirement for the products with close tolerances, high precision, and high surface quality in the fine grinding processes. In grinding processes, material removal occurs as shearing and ploughing combine to act. Therefore the material removal mechanism usually requires a higher specific energy which is high as compared with other machining processes [2]. The higher specific energy requirement in grinding process results in the higher heat generation which eventually induces the higher grinding zone temperature adversely affecting the ground surface quality of workpieces as well as the grinding wheel wear [3]. Such higher grinding zone surface temperature frequently results in the ground defects such as burning, oxidation, formation of untempered martensitic layer, induction of tensile residual stresses and cracks on the surface [4]. The most important aspect of improving the ground surface quality of workpieces is to use a high quality cooling lubricant system. It is effective that utilizing this system to remove the heat from the grinding zone and to reduce the friction between the workpiece and the grinding wheel. In general, metal cutting fluids (MCFs) are customarily used to control the cutting temperature in the cutting zone. Most lubricant types of the MCFs adopt the flooding, jet and mist form. But, the MCFs used in machining processes have been recently questioned due to adverse effects. Inappropriate disposal of MCFs results in the ground, water and air pollution, causing serious loss to the environment [5, 6]. The handling and disposal of MCFs must obey rigid rules of environmental protection agency. Consequently, decreasing use of MCFs not only abides by stricter environmental laws, but also reduces the costs of MCFs. The dry machining process, an environmentally friendly machining without the use of MCFs, is hardly required for higher machining efficiency, better surface finish quality, and severe cutting conditions [7]. Dry machining does not possess such environmental contaminant, but still cannot be completely accepted in the grinding processes.

A cold air gun coolant system was recently used in machining processes and produced a compressed cold air jet for cooling the workpiece and the cutting tool. Using the cooling

gas as a coolant offers the significant benefits: obtaining the desired cooling effect and being environmentally friendly all the while. Currently, there are several kinds of gases used as gas coolant such as air, nitrogen and carbon dioxide. The air is a free available natural resource and has no adverse effect on the health of the operator or the environment. Kishawy et al. [8] claimed that the surface roughness values for air cooling are higher than for fluid cooling in the end milling process. Sarma et al. [9] investigated the comparison of dry and air-cooled turning of grey cast iron tool with mixed oxide ceramic. At higher cutting speeds, the dry turning performs very poorly; hence, the air-cooled turning provides an improved surface finish and also significantly reduces the tool wear. Jerold and Kumar [10] used cryogenic carbon dioxide (CO2) as the cutting fluid while turning AISI 1045 steel. The efficiency of cryogenic CO2 compared to that of dry and wet machining presented to have satisfied improvements with respect to cutting temperature, cutting forces, chip disposal and surface roughness.

Ti–6Al–4V alloy is the most widely used titanium alloy due to its peculiar behavior and mechanical properties. Because it maintains high strength characteristic, high corrosion resistance and high fracture resistance even at elevated temperature, it has become to be a widely used material in manufactures of the aerospace, automotive, chemical and biomedical industries [11, 12]. Machining titanium alloy has been regarded as one of the most important manufacturing processes. Especially, for the advent of grinding the high strength titanium and nickel based super alloys, tremendous generated heat is accumulated in the grinding zone. Ti–6Al–4V alloy is classified as a difficult-to-machine material [13, 14]. Since it has low thermal conductivity, the accumulated heat in the grinding zone is unable rapidly scattered around. Most of the accumulated heat causes high and non-uniform temperatures in the grinding zone, involving the machined surface, the tiny grinding chip and the grinding wheel. These high and non-uniform temperatures may result in the surface damage of ground products such as burning and conjunction of high residual stresses. Meantime, they lead to the faster grinding wheel wear and thereby also affect the grinding wheel life and the quality and accuracy of the ground products. Therefore, it is an important issue to select a high quality cooling lubricant system in the grinding process of Ti-6Al-4V alloy.

The main objective of this paper is to present the mathematical models for modeling and optimizing the effects of processing parameters in order to investigate the machinability evaluation of cold air gun coolant system in the fine grinding process of Ti-6Al-4V alloy. In

this paper, an attempt made to model the machinability evaluation through the response surface methodology (RSM). The surface roughness, the morphology of ground surface and the chips formation were adopted to evaluate the machinability performances. The processing parameters, adopted form the significant processing parameters in the operation of cold air gun coolant system and the surface grinder, respectively, include the mass flow rate and the temperature of the cool air, wheel speed, feed rate and cutting depth of the fine grinding processes. The RSM is a collection of mathematical and statistical procedures that are useful for the modeling and the analysis of problems in which the response of demand is affected by several variables and the objective is to optimize this response [15, 16]. Through using the design of experiments and applying regression analysis, the modeling of the desiring response to several independent input variables can be gained. Consequentially, the RSM is utilized to describe and identify, with a great accuracy, the influence of the interactions of different independent variables on the response when they are varied simultaneously. In addition, it is one of the most widely used methods to solve the optimization problem in the manufacturing environments [17-21]. Therefore, the quadratic model of RSM associated with the sequential approximate optimization (SAO) method was used in an optimal setting of processing parameters, which may yield optimum machinability performances of Ti-6Al-4V alloy in the fine grinding process.

2. Experimental design and procedure

2.1 Experimental setup

In this study, the experimental setup for the fine grinding experiments is shown in Fig. 1. All the fine grinding experiments were conducted with cold air gun coolant system in a Chevalier PSG-518M surface grinder, which has a maximum spindle motor of 2 HP, grinding surface table size 146×460 mm, maximum manual travel of 180mm, hand-wheel per revolution of 3 mm, hand-wheel per graduation of 0.01 mm, and grinding speed of 3450-2850 rpm. For the present experimental studies, Ti–6Al–4V alloy was used as the workpiece material with a hardness of HRC 30–35. Its chemical composition is Al 6.5 wt.%, V 4.25 wt.%, Fe 0.04 wt.%, C 0.02 wt.%, N 0.015 wt.%, O 0.16 wt.%, H 0.0018 wt.%, Ti, and Bal. Its mechanical properties are density of 4.43 g/cm3, thermal conductivity of 5.44 Wm/K, Young’s modulus of 113 GPa, specific heat of 526.3 J/KgK, tensile strength of 993 MPa, yield strength of 861 MPa and Poisson’s ratio of 0.342. Prior to the grinding experiments, these workpieces were cut to be a rectangular block of 90×40×30 mm.

For investigating the air-cooling effect on the machinability performances of the fine grinding process, a cold air gun coolant system was adopted in the cooling status. The compressed cold air was provided by the cold air gun coolant system, which was composed of a vortex tube, a hot muffler and a cold muffler. The vortex tube system produces the cold and hot air from compressed air. The compressed air enters from the inlet hole into vortex tube. The vortex tube converts the compressed inlet air into two lower pressure air steams. These two air steams, cold and hot air, go through the cold and hot muffler into the ambient air, respectively. In Fig. 2, the cold air gun coolant system is shown in schematic form. In this figure, the controller is mounted on the hot muffler end to adjust cool air temperature, hot air temperature, hot and cool air stream mass flow rate simultaneously. In this study, the working condition of the vortex tube selected three statuses of temperature state and mass flow rate. The mass flow rate ($\dot{m}_A$) of the cold air was varied from 425 to 325 SLPM (standard liter per minute) and the temperature (T_A) of the cold air was varied from 5 to -5 ℃. The cold air stream was directed through the nozzle to provide an impinging jet between the grinding wheel and workpiece.

2.2 Experimental design

The real fine grinding processes of Ti-6Al-4V titanium alloy adopted two-stage process with a defined sparking-out regime coupled with a slow finishing feed rate. In order to visualize the effect of air-cooling, a series of fine grinding test were conducted as follows. The grain size of the grinding wheel (Aluminum oxide, WA60K3V1A) selected a 100–320 mesh grain for fine grinding. The wheel speed (V_S) adopted 3450 rpm; the feed rate (f) was varied between 22 and 6 m/min, and the cutting depth (α_P) was set from 0.001 to 0.015 mm. The setting of experimental parameters and instrument under grinding Ti–6Al–4V titanium alloy in the fine grinding processes is shown in Table 1. The values of selected range in Table 2 were based on the data of Machado and Wallbank [12] and practice machining results.

The value of surface roughness, morphology of ground surface and chips formation here was adopted as the machinability evaluation of Ti–6Al–4V titanium alloy ground in the fine grinding processes. The arithmetic mean roughness values, Ra, across the grinding direction have been measured at five different points of ground surface by using a Mitutoyo SurfTest-402. The morphology of ground surface and chips formation had been observed

using an optical microscope with magnification of 200 times.

In the cooling status, the mass flow rate ($\dot{m}_A$) and the temperature (T_A) of the cold air were actually chosen as two numerical factors for investigation. According to the previous analysis in the real grinding processes, the feed rate (f) and the cutting depth (α_P), were also chosen as two numerical factors. Table 2 shows the controllable parameters and their levels in the coded and actual values.

The experimental matrix adopted in the coded form is shown in Table 3. The coded values $X_{i,i=1,2,3,4}$ of the numerical factors used in Tables 2 and 3 were obtained from the following transformable equations:

$$X_1 = \frac{\dot{m}_A - \dot{m}_{A0}}{\Delta \dot{m}_A} \tag{1}$$

$$X_2 = \frac{T_A - T_{A0}}{\Delta T_A} \tag{2}$$

$$X_3 = \frac{f - f_0}{\Delta f} \tag{3}$$

$$X_4 = \frac{\alpha_P - \alpha_{P0}}{\Delta \alpha_P} \tag{4}$$

where X_1, X_2, X_3 and X_4 are the coded values of $\dot{m}_A$, T_A, f and a_p, respectively. $\dot{m}_{A0}$, T_{A0}, f_0 and a_{p0} are the values of $\dot{m}_A$, T_A, f and a_p at zero level. $\Delta \dot{m}_A$, ΔT_A, Δf and $\Delta \alpha_P$ are the intervals of variation in $\dot{m}_A$, T_A, f and a_p, respectively.

3. Mathematical modeling

The RSM is an empirical modeling approach for determining the relationship between various processing parameters and responses with the various desired criteria and searches for the significance of these process parameters in the coupled responses [17-21]. It is a sequential experimentation strategy for building and optimizing the empirical model. Therefore, RSM is a collection of mathematical and statistical procedures, and is good for the modeling and analysis of problems in which the desired response is affected by several variables. The mathematical model of the desired response to several independent input variables is gained by using the experimental design and applying regression analysis.

In this study, the quantitative form of relationship between the desired response and

independent input variables can be represented in the following:

$$Y = F(\dot{m}_A, T_A, f, \alpha_P) \tag{5}$$

where Y is the desired response and F is the response function (or response surface). In this particular case, the approximation of Y was proposed by using the fitted second order polynomial regression model which is called the quadratic model. The quadratic model was exactly suitable for studying carefully the interactive effects of combinative factors on the performance evaluations. The quadratic model of Y can be written as follows:

$$Y = a_0 + \sum_{i=1}^{4} a_i X_i + \sum_{i=1}^{4} a_{ii} X_i^2 + \sum_{i<j}^{4} a_{ij} X_i X_j \tag{6}$$

where a_0 is constant, a_i, a_{ii} and a_{ij} represent the coefficients of linear, quadratic and cross product terms, respectively. This model using the quadratic model of F in this study not only aims to investigate the response over the entire factor space, but also to locate the region of desired target where the response approaches to its optimum or is near to optimal value. In general, the quadratic model of desired response (Y) can be expressed in the matrix form as follows :

$$\mathbf{Y} = \mathbf{X}\boldsymbol{\alpha} + \boldsymbol{\varepsilon} \tag{7}$$

where $\mathbf{X}$ is a matrix of model terms evaluated at the data points, $\boldsymbol{\varepsilon}$ is an error vector. The unbiased estimator $\boldsymbol{\varepsilon}$ of the regression coefficient vector $\boldsymbol{\alpha}$ is estimated by using the least-squares error method as follows.

$$\boldsymbol{\alpha} = (\mathbf{X}^{\mathbf{T}}\mathbf{X})^{-1}\mathbf{X}^{\mathbf{T}}\mathbf{Y} \tag{8}$$

where $\mathbf{X}^{\mathbf{T}}$ is the transpose of the matrix $\mathbf{X}$.

In this study, the approximation of the mathematical model will be proposed using the fitted second-order polynomial regression model, which is called the quadratic model. The necessary data for building the response model are generally collected by the experimental design. In this study, the experimental design adopts the centered central composite design (CCD) in order to fit the quadratic model of the RSM. The factorial portion of CCD is a full factorial design with all combinations of the factors at two levels (high, +1 and low, −1) and composed of the eight star points, and six central points (coded level 0) which is the midpoint between the high and low levels. The star points are at the face of the cube portion on the design which corresponds to an α value of 1. This type of design is commonly called

the face-centered CCD. The experimental plan is generated using the stipulated conditions based on the face centered CCD and involves 30 runs as shown in Table 3. Each combination of experiments will be repeated three times under the same conditions at different times to acquire a more accurate result in this process. The arithmetic mean roughness value, Ra, indicated as Y , was analyzed as response.

Consequently, the RSM is a sequential procedure and its procedure for determining the machining parameters with optimal performance characteristics, including seven steps, is summarized in the following:

(1) Defining the independent input variables and desired responses with the design constraints
(2) Adopting the face-centered CCD to plan the experimental design
(3) Performing the regression analysis with the quadratic model of RSM
(4) Calculating the statistical analysis of variance (ANOVA) for the independent input variables and finding out which parameter significantly affects the desired response
(5) Determining the situation of the quadratic model of the RSM and deciding whether the model of the RSM needs screening variables or not
(6) Obtaining the optimal machining parameters with the design constraints using the SAO method
(7) Conducting confirmation experiment and verifying the optimal machining parameters setting

4. Results and discussion

4.1 The status of ground surface and chips formation

The most important aspect of improving the quality of ground surface is to use a high quality cooling lubricant. Figure 3 displays the morphology analysis and quality of ground surfaces in the dry and air-cooled grinding processes, respectively. The surface damages including the plastic deformation, side flow and grain pull-out were observed to be severe in the dry grinding processes. These conditions lead to the increasing of material elastic-plastic deformation and ploughing phenomenon. Using the compressed cold air presents better penetration of the cooling and lubricant effects to the underside of the ground interface, which results in lowering the friction and reducing the adhesion of the work material. Therefore, the growth of surface damages is minimized in air-cooled grinding processes.

Figure 4 reveals the images of the chips obtained as the chips were formed under the same grinding conditions in the dry and air-cooled grinding processes, respectively. The chips formation is subjected to the effect of friction, the cutting edges conditions and flow properties of materials. In the case of dry condition, it shows that the metal ground would produce thick types and long chips. The chip breakability is good under air-cooled condition when compared with itself in dry grinding process. It can be seen that the fragile and thin chips are produced under the air-cooling process. This event attributed that the compressed cold air presents better penetration of the cooling and lubricant to the underside of the ground interface, which causes the lower friction and reduces the adhesion of the work material. This status causes the dramatic increase in brittleness at lower temperature, and easily produces the fragile and thin chips.

4.2 Modeling of surface roughness in the ground surface

The surface roughness in the ground surface regarded as an important performance characteristic, was adopted to investigate the machinability evaluation of cold air gun coolant system in the fine grinding process of Ti-6Al-4V alloy. The 30 experimental runs were conducted in duplicate, and the average values of surface roughness *Ra* (Y , μm) along with the design matrix are listed in Table 3.

From the results of Table 4, the values obtained were as follows: R^2=0.9469, R^2 Adjusted=0.8974, and AP=18.58 for the average values of surface roughness Ra (Y , μm). The adjusted R-squared (R2 Adjusted) presents a measure of the amount of variation around the mean explained by the model, adjusted for the number of terms in the model. The adjusted R-squared (R^2 Adjusted) decreases as the number of terms in the model increases if those additional terms don't add value to the model. Furthermore, the value of adequate precision (AP) in this model, which compares the range of the predicted value at the design point to the average prediction error, is well above 4. The value of the ratio is greater than 4, which presents the adequate model discrimination. These models obtain higher values of the R^2, R^2 Adjusted and AP at the same time. Consequently, the obtained quadratic mathematical models for the average values of surface roughness *Ra* (Y , μm) can be regarded as significant effect for fitting and predicting the experimental results, and meantime, the test of lack-of-fit also displays to be insignificant.

Table 5 shows that the values of "F value"' and "Prob. >F" for each term on the

performances of the disintegration factor (FD). The $X_1(\dot{m}_A)$, $X_2(T_A)$, $X_3(f)$, $X_4(a_p)$, X_1X_4, X_2X_3, X_2^2, and X_4^2 can be regarded as significant terms because their "Prob. > F" values are <0.05. The backward elimination process eliminates the insignificant terms to adjust the fitted quadratic models. These insignificant model terms can be removed, and the test of lack-of-fit also displays to be insignificant. Through the backward elimination process, the final quadratic models of response equation in terms of coded factors are presented as follows:

$$\begin{aligned} Y \; &= 0.287 - 0.042\,X_1 + 0.019\,X_2 - 0.032\,X_3 \\ &\quad + 0.021\,X_4 - 0.005\,X_1X_4 + 0.004\,X_2X_3 \\ &\quad + 0.024\,X_2^{\,2} + 0.023\,X_4^{\,2} \end{aligned} \tag{9}$$

In terms of actual factors the final quadratic models of response equation are as follows:

$$\begin{aligned} Ra = {} & 0.632 - 6.3\times10^{-4}\,\dot{m}_A + 2.358\times10^{-3}\,T_A - \\ & 4.031\times10^{-3}\,f - 6.325\,\alpha_P - 0.022\,\dot{m}_A\alpha_P \\ & + 1.093\times10^{-4}\,T_A f + 9.551\times10^{-4}\,T_A^{\,2} + 954.838\,\alpha_P^2 \end{aligned} \tag{10}$$

The results of comparison prove that the predicted values of surface roughness (*Ra*) are close to those readings recorded in the experiment with a 95% confidence interval.

4.3 The machinability evaluation of cold air gun coolant system

In the fine grinding process, the mass flow rate ($\dot{m}_A$) and the temperature (T_A) of the cold air, the feed rate (f) and the cutting depth (α_P) were chosen as the three numerical factors so as to investigate the influences on the surface roughness (*Ra*) in the ground surface. The influences of machining parameters on the performance of the surface roughness had been analyzed, which was based on the mathematical model proposed above in Section 4.2.

Figure 5 shows the response surface and contour plot for the values of surface roughness (*Ra*) in relation to the mass flow rate ($\dot{m}_A$) of the cold air and the feed rate (f). The other two parameters, the temperature (T_A) of the cold air and the cutting depth (α_P), maintained at the middle levels and were set to be 0 ^{o}C and 0.010mm, respectively, under the fine grinding process. First, it can be seen that the tendency of =surface roughness value

(*Ra*) obviously decreases with the increase of the mass flow rate under the air-cooled grinding process. This event shows that the cold air in the gas form has better penetration in the grinding zone than any conventional coolants in the grinding process. Therefore, by increasing the mass flow rate of the cold air, this presents the good effects of cooling and lubrication between the grinding wheel and the ground surface, and causes the lower friction and reduces the adhesion of the work material. Consequently, this status easily produces the best quality of the ground surface. In addition, from Fig. 5, it also can be seen that the tendency of surface roughness values (*Ra*) decreases with the increase of feed rate.

Figure 6 depicts the response surface and contour plot for the values of surface roughness (*Ra*) in relation to the mass flow rate ($\dot{m}_A$) of the cold air and the cutting depth (α_P). The other two parameters, the temperature (T_A) of the cold air and the feed rate (f) maintained at the middle levels, were set to be 0 ^{o}C and 14 m/min, respectively, under the fine grinding process. As the result of Fig. 6, it also can be obviously seen that the tendency of surface roughness value (*Ra*) decreases with the increase of the mass flow rate under the air-cooled grinding process. In general, the utility of air-cooling process improves the efficiency of heat removal and diffusion, especially in the type of force convection. It also advantages the good effects of cooling and lubrication between the grinding wheel and the ground surface. But, as the cutting depth increases, the general trend of the increase in the surface roughness (*Ra*) with the increase in the cutting depth is clearly observed at the high value of cutting speed. This result has been attributed to the promotion of resistance forces at the grain of the grinding wheel, which easily generates the fragile and thin chips, thus results in the growth of surface damages.

In this study, the utility of air-cooling process adopted the control method of the mass flow rate ($\dot{m}_A$) and the temperature (T_A) of the cold air. Figure 7 displays the response surface and contour plot for the values of surface roughness (Ra) in relation to the temperature (T_A) of the cold air and the feed rate (f). The other two parameters, the mass flow rate ($\dot{m}_A$) of the cold air and the cutting depth (α_P) maintained at the middle levels, were set to be 375 SLPM and 0.010mm, respectively, under the fine grinding process. It can be noticed that the tendency of the values of surface roughness (*Ra*) decreases with the decrease of the cold air temperature under the air-cooled grinding process. This event shows that the decrease of the cold air temperature presents the good effects of cooling between the grinding wheel and the ground surface, and easily produces the best quality of the

ground surface. From Fig. 7, it also can be noticed that the tendency of the values of surface roughness (Ra) decreases with the increase of feed rate.

Figure 8 presents the response surface and contour plot for the values of surface roughness (Ra) in relation to the temperature (T_A) of the cold air and the cutting depth (α_P). The other two parameters, the mass flow rate ($\dot{m}_A$) of the cold air and the feed rate (f) maintained at the middle levels, were set as 375 SLPM and 14 m/min, respectively, in the fine grinding process. As the result of Fig. 8, it also can be observed that the tendency of surface roughness value (Ra) decreases with the decrease of the cold air temperature under the air-cooled grinding process. As the cutting depth increases, the general trend of the increase in the surface roughness (Ra) with the increase in the cutting depth is clearly observed at the high value of cutting speed.

Comparing the results of Figs 5, 6, 7 and 8, it can be observed that the tendency of the surface roughness (Ra) is more obvious decrease with the increase of the mass flow rate than with the decrease of the cold air temperature. Figure 9 shows the response surface and contour plot for the values of surface roughness (*Ra*) in relation to the mass flow rate ($\dot{m}_A$) and the temperature (T_A) of the cold air. The other two parameters, the feed rate (f) and the cutting depth (α_P) maintained at the middle levels, were set to be 14 m/min and 0.010mm, respectively, in the fine grinding process. From the result of Fig. 9, it can be confirmed that the tendency of the values of surface roughness (*Ra*) obviously decreases with the increase of the cold air mass flow rate and the decrease of cold air temperature. This event approves that the cold air in the gas form has better penetration in the grinding zone than any conventional coolants in the grinding process and results in the good effects of cooling and lubrication between the grinding wheel and the ground surface, and easily produces the best quality of the ground surface. In addition, from Fig. 9, the tendency of the surface roughness (*Ra*) is more obvious decrease with the increase of the cold air mass flow rate than with the decrease of the cold air temperature.

4.4 Optimization of processing parameters

The goal of optimization for the fine grinding process subjected to a set of processing constrains in this study is to find the optimal values of processing parameters (*X*) in order to minimize the value of roughness value, *Ra*. Therefore, this optimization problem can be approximated by the following equations:

Find $X = [\dot{m}_A, T_A, f, \alpha_P]$ (11)

to minimize $f(X) = Ra$ (12)

Subject to $325 \le \dot{m}_A \le 425$ SLPM, $-5 \le T_A \le 5$ ℃ (13a)

$6 \le f \le 22$ m/min, $0.001 \le \alpha_P \le 0.005$ mm (13b)

In the present investigation, the constrained optimization problem was solved by means of a sequential approximate optimization (SAO) method. This method makes use of an objective function, *f(X)*, called the desirability function. It reflects the desirable ranges for each response. For simultaneous optimization each response must have a low and high value assigned to each goal. The SAO strategy in the RSM applies the approximate procedure, which is iteratively repeated until convergence. The corresponding optimal grinding conditions found by the SAO method were presented in Table 5. The optimum processing parameters obtained in Table 6 are found to be feed rate (f) of 20.96 m/min, cutting depth (α_P) of 0.005 mm, cold air mass flow rate ($\dot{m}_A$) of 406.60 SLPM and cold air temperature (T_A) of -4.97 ^{o}C. From the optimization results in Table 5, it is seen that the minimum surface roughness value is 0.24 μm that has a good agreement with result of experiment. As shown in Table 6, the optimized surface roughness (*Ra*) represents a reduction of 24.86% compared to the initial surface roughness *Ra* of 0.31 μm.

4.5 Confirmation experiments

In order to verify the adequacy of the quadratic model obtained, the confirmation run experiment for the obtained optimum processing parameters was performed for the surface roughness (*Ra*). The data from the confirmation run and their comparisons with the predicted values for the surface roughness (*Ra*) are illustrated in Figure 10. The residual and the percentage error calculated are small. The percentage errors between the experimental and predicted value of *Ra* are -0.41%. All the experimental values for the confirmation run are within the 95% prediction interval. Obviously, the quadratic model obtained is excellently accurate.

5. Conclusions

The conclusions of research are as follows:

(1) The cold air gun coolant system has better penetration in the grinding zone, and presents the good effects of cooling and lubrication between the grinding wheel and the ground

surface. It reduces the growth of surface damages and easily produces the fragile and thin chips.

(2) The results of ANOVA and the comparisons of experimental data show that the mathematical model of the surface roughness (Ra) is fairly well-fitted for the experimental values with a 95% confidence interval.

(3) The tendency of surface roughness value (Ra) obviously decreases with the increase of the cold air mass flow rate and the decrease of cold air temperature.

(4) The obtained optimal grinding conditions provide the optimized surface roughness value (Ra) which represents a reduction of 24.86% compared to the initial surface roughness.

References

[1] Shaw, M.C. (1996). Principles of abrasive processing. Oxford University Press, New York.

[2] Malkin, S., Guo, C. (2008). Grinding technology, theory and applications of Machining with Abrasives. Industrial Press, NewYork.

[3] Anderson, S., Malkin, R.B. (1974). Thermal aspects of grinding-Part 1. Energy partitioning. Int J Eng 96: 1177-1183.

[4] Snoeys, R., Maris, M., & Peters, B.J. (1978). Thermally induced damages in grinding. Ann. ClRP 27: 571-581.

[5] Byrne, G., Scholta, E. (1993). Environmentally clean machining processes—a strategic approach. Ann CIRP 42(1):471–474.

[6] Sokovic, M., Mijanovic, K. (2001). Ecological aspects of the cutting fluids and its influence on quantifiable parameters of the cutting processes. J Mater Process Technol 109(1–2):181–189.

[7] Sreejith, P.S., Ngoi, B.K.A. (2000). Dry machining: machining the future. J Mater Process Technol 101(1):287–291.

[8] Kishawy, H.A., Dumitrescu, M., Ng, E.G., & Elbestawi, M.A. (2005). Effect of cooling strategy on tool performance, chip morphology and surface quality during high speed machining of A356 aluminum alloy. Int J Mach Tool Manuf 45:219–227.

[9] Sarma, D.K., Dixit, U.S. (2007). A comparison of dry and air-cooled turning of greycast iron with mixed oxide ceramic tool. Mater Process Technol 190: 160–172.

[10] Jerold, B. D., Kumar, M. P. (2011). Experimental investigation of turning AISI 1045

steel using cryogenic carbon dioxide as the cutting fluid. J Manuf Proces 13: 113–119.

[11] Yalçın, B., Özgür, A.E., Koru, M. (2009). The effects of various cooling strategies on surface roughness and tool wear during soft materials milling. Mater Des 30:896–899.

[12] Machado, A.R., Wallbank, J. (1990). Machining of titanium and its alloys—a review. Proc Inst Mech Eng 204:53–60.

[13] Ezugwu, E.O., Wang, Z.M. (1998). Titanium alloys and their machinability—a review. J Mater Process Technol 68:262–274.

[14] Arrazola, P.J., Garay, A., Iriarte, L.M., Armendia ,M., Marya, S., & Le Maitre, F. (2009). Machinability of titanium alloys. J Mater Process Technol 209:2223–2230.

[15] Myers, R.H., Montgomery, D.C. (1995). Response surface methodology: Process and product optimization using designed experiments. John Wiley & Sons, New York.

[16] Montgomery, D.C. (2001). Design and Analysis of Experiments. John Wiley & Sons, New York.

[17] Grum, J., Slab, J.M. (2004). The use of factorial design and response surface methodology for fast determination of optimal heat treatment conditions of different Ni–Co–Mo surface layers. J Mater Process Technol 155/156: 2026–2032.

[18] Puri, A.B., Bhattacharyya, B. (2005). Modeling and analysis of white layer depth in a wire-cut EDM process through response surface methodology. Int J Mach Tools Manuf 25: 301–307.

[19] Ozcelik, B., Erzurmlu, T. (2005). Determination of effecting dimensional parameters on warpage of thin shell plastic parts using integrated response surface method and genetic algorithm. Int Commun Heat Mass Transfer 32: 1085–1094.

[20] Kansal, H.K., Singh, S., Kumar, P. (2005) Parametric optimization of powder mixed electrical discharge machining by response surface methodology. J Mater Process Technol 169: 427–436.

[21] Oktem, H., Erzurmlu, T., & Kurtaran, H. (2005). Application of response surface methodology in the optimization of cutting conditions for surface roughness. J Mater Process Technol 170: 11–16.

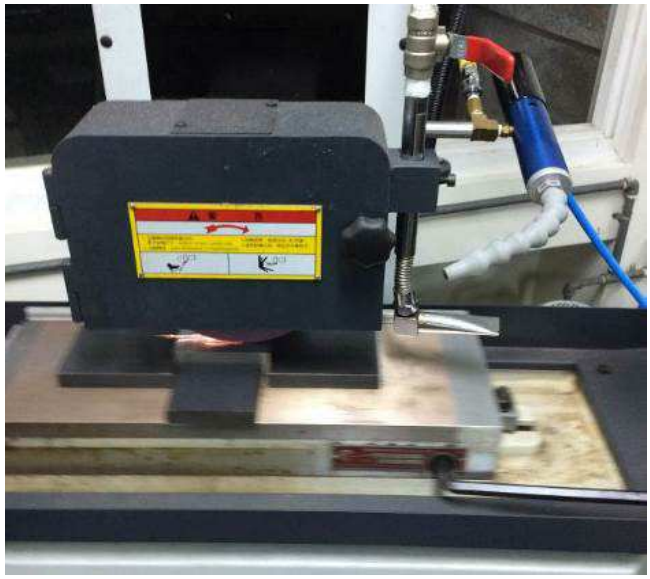

Fig. 1 Schematic diagram of the experimental setup for the fine grinding experiments

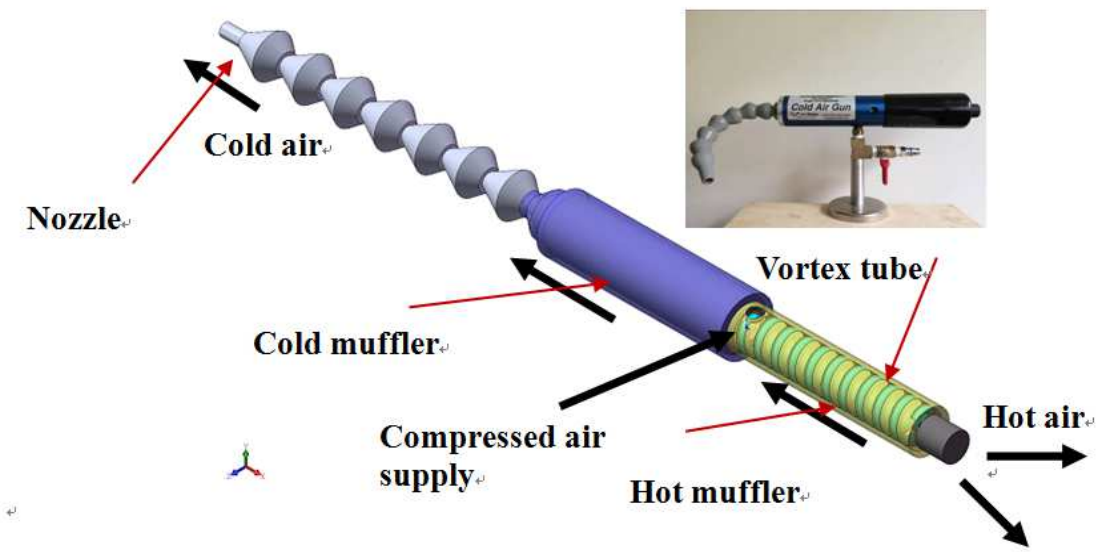

Fig. 2 Schematic diagram of the cold air coolant gun system

(a)

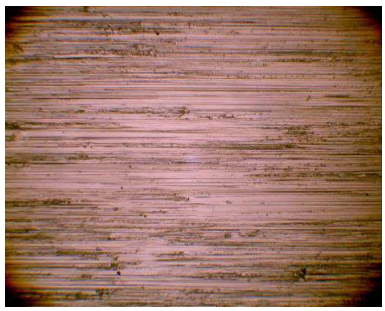

(b)

Fig. 3 The morphology analysis and quality of ground surfaces in the (a) dry and (b) air-cooled grinding processes

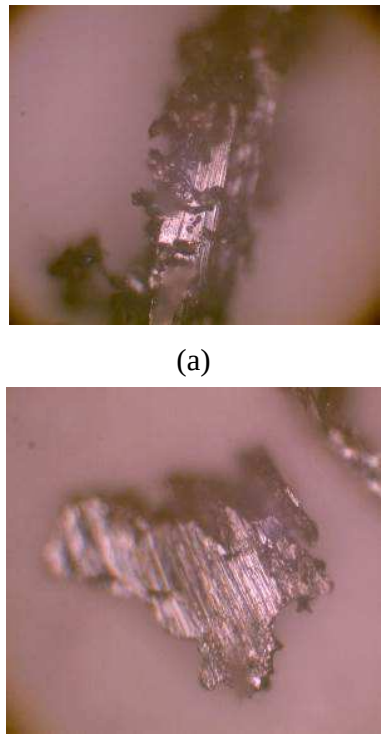

(a)

(b)

Fig. 4 The images of the chips in the (a) dry and (b) air-cooled grinding processes

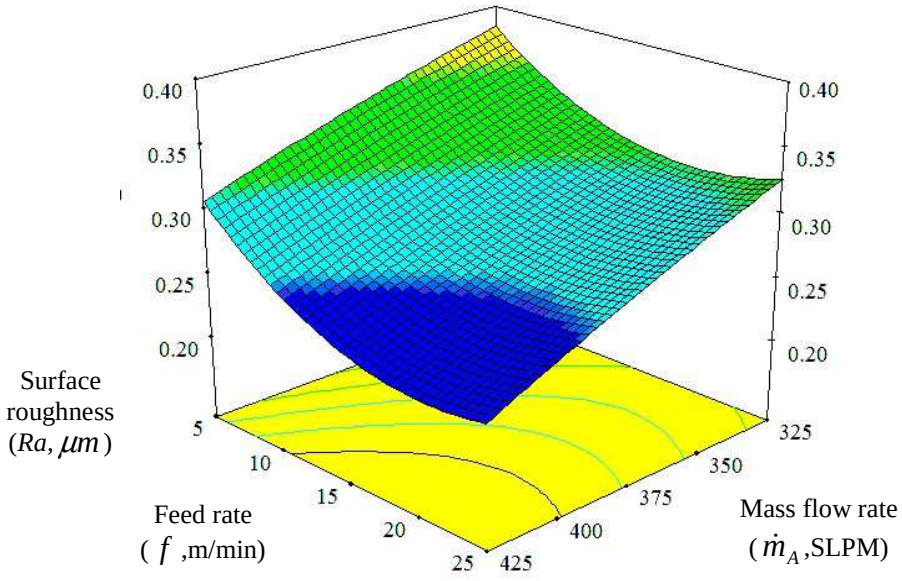

Fig. 5 The response surface and contour plot for the values of surface roughness (*Ra*) in relation to the mass flow rate ($\dot{m}_A$) of the cold air and the feed rate (f).(T_A=0 ºC, α_P = 0.010mm)

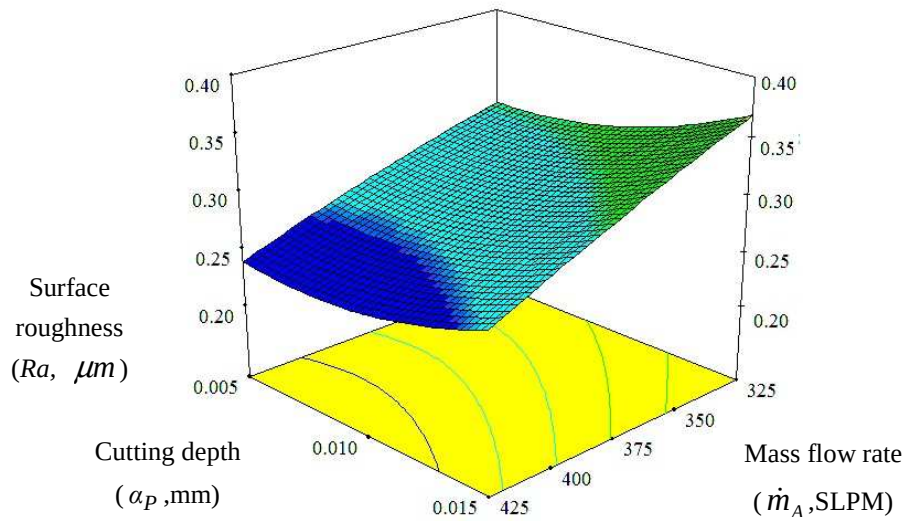

Fig. 6 The response surface and contour plot for the values of surface roughness (*Ra*) in relation to the mass flow rate ($\dot{m}_A$) of the cold air and the cutting depth (α_P). (T_A=0 ºC, f =14 m/min)

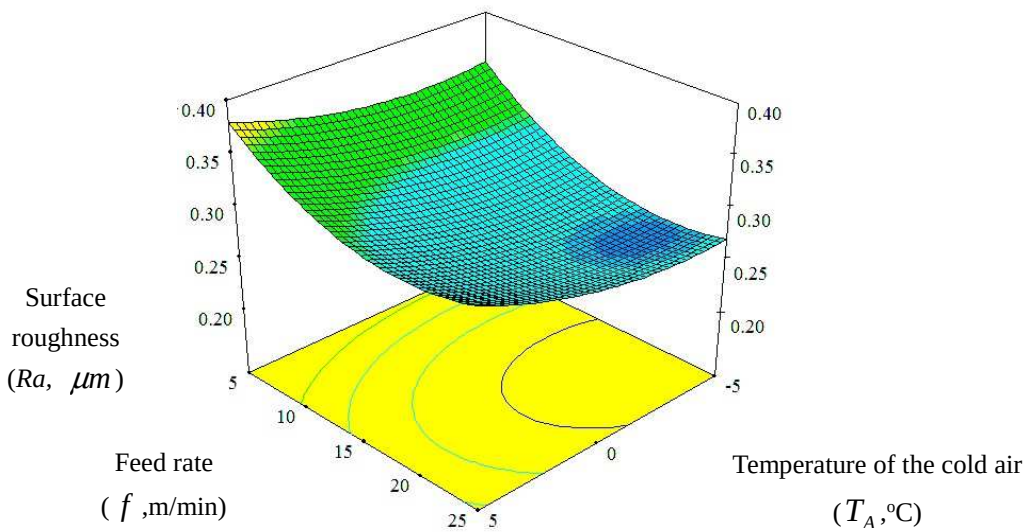

Fig. 7 The response surface and contour plot for the values of surface roughness (Ra) in relation to the temperature (T_A) of the cold air and the feed rate (f). ($\dot{m}_A$=375 SLPM, α_P = 0.010mm)

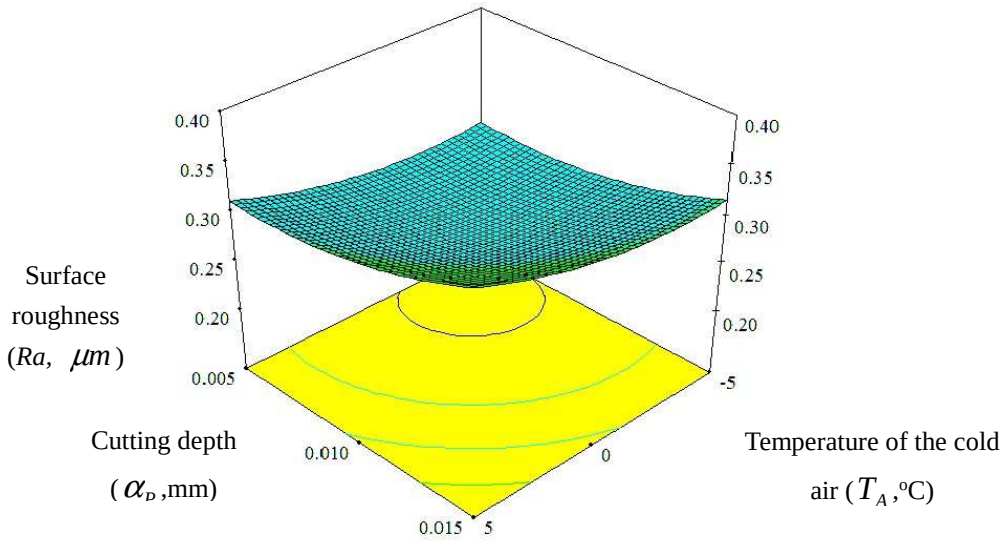

Fig. 8 The response surface and contour plot for the values of surface roughness (*Ra*) in relation to the temperature (T_A) of the cold air and the cutting depth (α_P). ($\dot{m}_A$=375 SLPM, f =14 m/min)

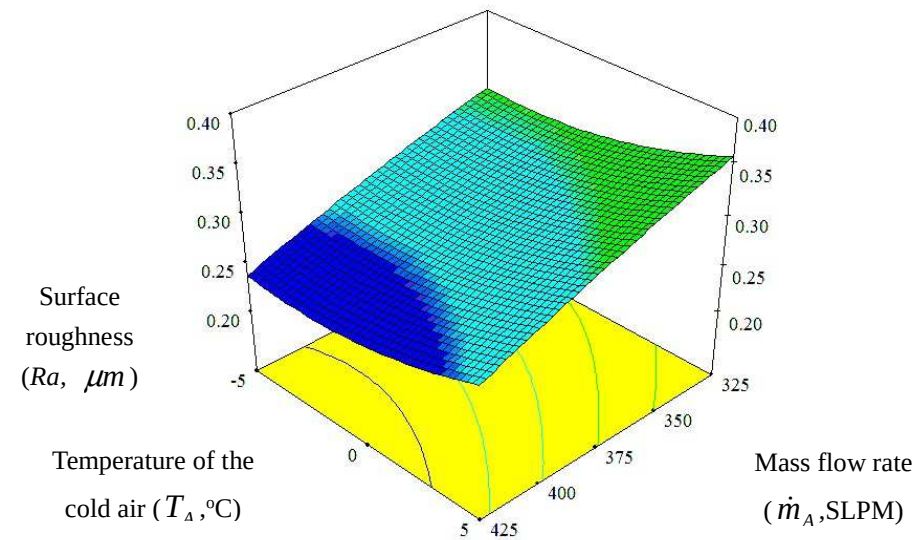

Fig. 9 The response surface and contour plot for the values of surface roughness (*Ra*) in relation to the mass flow rate ($\dot{m}_A$) and the temperature (T_A) of the cold air. (f =14 m/min, α_P = 0.010mm)

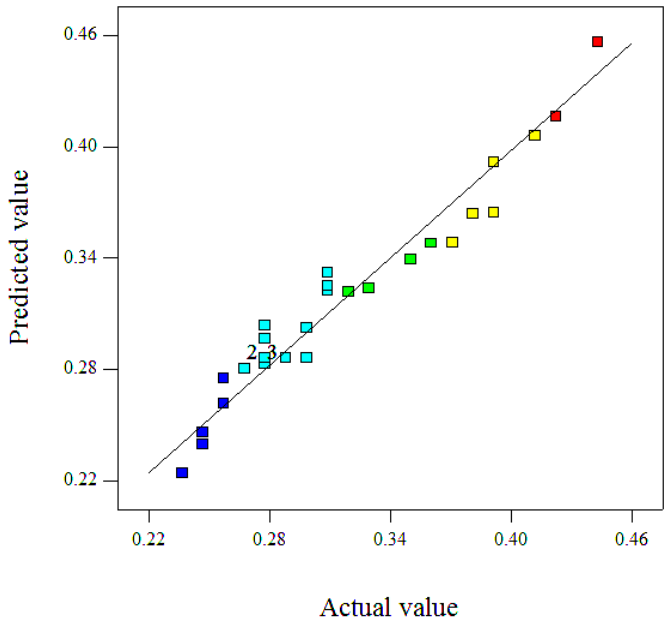

Fig. 10 The comparisons of the actual value and the predicted values for the surface roughness (*Ra*).

Table 1 Experimental conditions

Grinding machine	Chevalier FSG-618 surface grinder
Workpiece material	Ti–6Al–4V alloy
Dimensions of workpiece	90×40×30 mm rectangular block
Grinding mode	Plunge surface grinding, down cut
Grinding wheel	Aluminum oxide (WA60K3V1A)
Grinding conditions	
Wheel speed (V_S)	3450 rpm
Feed rate (f)	22, 14, 6 m/min
Cutting depth (α_P)	0.005, 0.010, 0.015 mm.
Coolant-lubricant environment	Compressed cold air
Cold air gun coolant system	
mass flow rate ($\dot{m}_A$)	325, 375, 425 SLPM
Temperature (T_A)	5, 0, -5 °C
Air pressure	7.0 bar

Table 2 Design schema of machining parameters and their levels

Parameters		Levels		
		1	2	3
	Code	− 1	0	+1
Mass flow rate of cold air ($\dot{m}_A$, SLPM)	X_1	325	375	425
Temperature of cold air (T_A, ℃)	X_2	-5	0	5
Feed rate (f, m/min)	X_3	6	14	22
Depth of cut (α_P, mm)	X_4	0.005	0.010	0.015

Table 3 Design layout and experimental results

Run	Coded factors				Actual factors				Responses	
	Mass flow rate	Temperature	Feed rate	Cutting depth	Mass flow rate	Temperature	Feed rate	Cutting depth	Actual value	Predicted value
	X_1	X_2	X_3	X_4	$\dot{m}_A$	T_A	f	α_P	Ra (Y, μm)	Ra (μm)
1	0	0	0	+1	375	0	14	0.015	0.38	0.36
2	+1	–1	+1	+1	425	-5	22	0.015	0.3	0.3
3	+1	–1	–1	+1	425	-5	6	0.015	0.39	0.39
4	+1	+1	–1	–1	425	5	6	0.005	0.31	0.32
5	0	0	0	0	375	0	14	0.010	0.28	0.3
6	–1	–1	+1	–1	325	-5	22	0.005	0.24	0.22
7	+1	+1	–1	+1	425	5	6	0.015	0.37	0.35
8	+1	0	0	0	425	0	14	0.010	0.26	0.26
9	0	0	0	0	375	0	14	0.010	0.42	0.42
10	–1	0	0	0	325	0	14	0.010	0.31	0.33
11	0	0	0	0	375	0	14	0.010	0.44	0.46
12	+1	–1	+1	–1	425	-5	22	0.005	0.39	0.36
13	–1	+1	+1	+1	325	5	22	0.015	0.36	0.35
14	+1	–1	–1	–1	425	-5	6	0.005	0.25	0.25
15	0	+1	0	0	375	5	14	0.010	0.41	0.41
16	–1	+1	–1	–1	325	5	6	0.005	0.28	0.3
17	+1	+1	+1	–1	425	5	22	0.005	0.31	0.33
18	+1	+1	+1	+1	425	5	22	0.015	0.25	0.24
19	–1	–1	–1	+1	325	-5	6	0.015	0.28	0.28

20	–1	–1	+1	+1	325	-5	22	0.015	0.32	0.32
21	–1	+1	+1	–1	325	5	22	0.005	0.35	0.34
22	0	0	0	0	375	0	14	0.010	0.26	0.28
23	–1	–1	–1	–1	325	-5	6	0.005	0.27	0.28
24	0	0	0	0	375	0	14	0.010	0.33	0.32
25	0	–1	0	0	375	-5	14	0.010	0.29	0.29
26	–1	+1	–1	+1	325	5	6	0.015	0.3	0.29
27	0	0	0	–1	375	0	14	0.005	0.28	0.29
28	0	0	+1	0	375	0	22	0.010	0.28	0.29
29	0	0	–1	0	375	0	6	0.010	0.29	0.29
30	0	0	0	0	375	0	14	0.010	0.29	0.29

Table 4 The ANOVA for the fitted models

Final quadratic models	Roughness, Ra (Y)
F-Value	19.12
Prob. > F	< 0.0001
R^2	0.9469
R^2 Adjusted	0.8974
Adequate precision (AP)	18.58
Lack of Fit	not significant

Table 5 Results of the ANOVA

Symbol	Degree of freedom	Disintegration factor (F_D)	
		F-value	Prob. > F
$X_1(\dot{m}_A)$	1	105.434	< 0.0001*
$X_2(T_A)$	1	21.783	0.0003*
$X_3(f)$	1	59.821	< 0.0001*
$X_4(\alpha_P)$	1	27.047	0.0001*
X_1X_2	1	0.180	0.6774
X_1X_3	1	18.280	0.0374
X_1X_4	1	1.620	0.0024*
X_2X_3	1	19.980	0.0378*
X_2X_4	1	0.500	0.4903
X_3X_4	1	0.180	0.6774
X_1^2	1	0.107	0.7478
X_2^2	1	6.371	0.0197*
X_3^2	1	3.799	0.0702
X_4^2	1	6.372	0.0196*
Residual	15		
Total	29		

*indicates the significant term